Exact computation of waterhammer in a three-reservoir system

Arris S. TIJSSELING
Department of Mathematics and Computer Science
Eindhoven University of Technology, The Netherlands

Anton BERGANT
Litostroj Power d.o.o.
Ljubljana, Slovenia

ABSTRACT

The three-reservoir problem is a classic topic in hydraulic engineering. Three pipelines connect three reservoirs at a common junction. The three reservoirs have different elevations and liquid flows from the highest to the lowest reservoir. The main question is: will liquid flow to or from the middle reservoir? The classic problem concerns the calculation of the steady flow rates and hydraulic grade lines in the system. The present paper focuses on unsteady flow in the system. A simple and elegant method is presented that is able to detect exactly all reflections and transmissions of pressure waves at the three-way junction.

1 INTRODUCTION

The first illustration of a three-reservoir system known to the authors is shown in Fig. 1. It is copied from a 19th century paper by no one less than Coriolis (Ref. 1) in which he analyses a hydraulic machine invented by de Caligny (Refs. 2-4). The machine is intended to transport water from the lower reservoir (A) to the highest reservoir (G). As indicated by de Caligny (Ref. 3), it is based and related on previous inventions by Heron of Alexandria (first century B.C), Denizard and de La Deuille (1726), Manoury d'Ectot (1812) and makes use of mass oscillations. This is in contrast with the hydraulic ram invented by Whitehurst (1775) and Montgolfier (1797), which fully exploits waterhammer to elevate water to a higher level (Refs. 5-10). In hydro-power stations the typical three-reservoir system consists of pressure tunnel, penstock and surge shaft (Ref. 11) and – different from the "classical" three-reservoir system – it is not only the steady state but also the unsteady state that is of importance. The time scales of the system (response times and natural periods) and the excitation will tell us whether the flow can be considered as steady, unsteady rigid or unsteady elastic (Refs. 12-13).

Exact three-reservoir solutions – in addition to known exact solutions for steady flow and mass oscillation – for frictionless waterhammer are the goal and the new element of this paper. To this end an alternative way of waterhammer computation is applied. The procedure is based on the method of characteristics, but a computational grid is not required. Any point in the distance-time plane can be selected to compute the local-instantaneous solution without explicitly using stored previous solutions. The computation is based on automatically back-tracking pressure waves by means of a very simple recursion, so that the required programming effort is small. Exact solutions are thus obtained for frictionless waterhammer and for waterhammer with friction lumped at the pipe ends. Arbitrary initial conditions and time-dependent linear or quadratic boundary conditions are permitted. Exact solutions obtained for pressure surges in a three-reservoir system are compared with conventional waterhammer calculations. The exact solutions can be used to assess the numerical error in more conventional methods. The intriguing mathematical issue of an exponentially growing number of travelling wave fronts – due to wave reflection and transmission at the junction – is addressed.

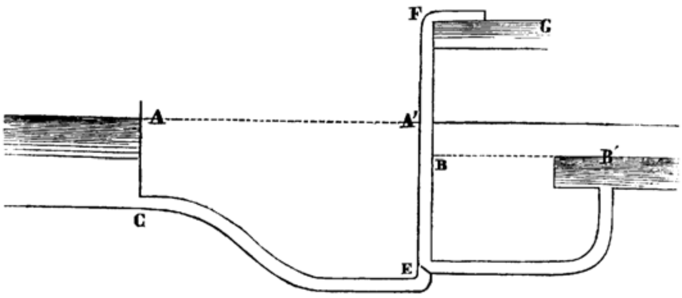

Figure 1. Three-reservoir system by Coriolis (1838).

2 THREE-RESERVOIR PROBLEM

The modelled system consists of three pipes of different lengths L, different diameters D and different Darcy-Weisbach friction factors f. The friction factors are taken constant herein, although in reality they vary somewhat with the flow velocity V. Each pipe is at one end connected to a reservoir of given elevation and at the other end to a three-way junction, as sketched in Fig. 2. Reservoir 1 has the highest elevation and Reservoir 2 the lowest, so that steady flow is always from Reservoir 1 to Reservoir 2. The direction of flow in Pipe 3 is not known in advance. A valve is located at the downstream end of Pipe 2. Manipulation of this valve generates unsteady flow.

The reference level of elevation is at the junction and the different elevations z of the reservoirs are included in $P := p + \rho g z$, where p is pressure. Numeral subscripts i are used to indicate the three pipes and the three reservoirs. The flow and x-coordinate directions are positive out of Reservoir 1 and towards Reservoirs 2 and 3. The pressure at the junction, where $z = 0$, is denoted by P_J. Minor losses at the junction are disregarded.

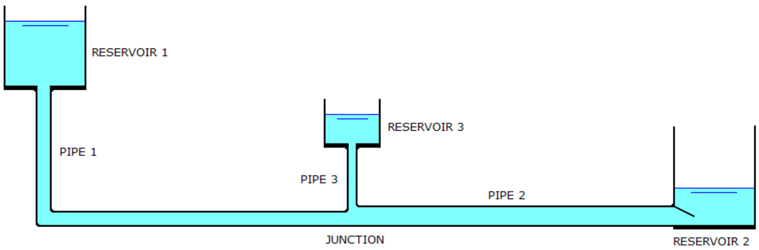

Figure 2. Sketch of the three-reservoir system studied herein.

3 EXACT STEADY-FLOW SOLUTION

If there are no changes to the system, the time scale of change is infinite and the flows are steady. The four algebraic equations governing the four unknowns V_1, V_2, V_3 and P_J are:

$$P_1 - P_J = f_1 \frac{L_1}{D_1} \frac{\rho V_1^2}{2} \ ,$$

$$P_J - P_2 = f_2 \frac{L_2}{D_2} \frac{\rho V_2^2}{2} \ ,$$

$$P_J - P_3 = f_3 \frac{L_3}{D_3} \frac{\rho V_3 |V_3|}{2} \ ,$$

$$A_1 V_1 = A_2 V_2 + A_3 V_3 \ , \quad \text{with} \ A_i = \frac{\pi D_i^2}{4} \ . \tag{1}$$

It is a straightforward exercise to solve these equations symbolically (Refs. 14-16). The constant velocities V_1, V_2, V_3 and the corresponding linearly decreasing "pressures" P can be used as input for rigid-column and waterhammer calculations. These solutions also describe quasi-steady flows, where the excitation time scale is larger than $2D/(f\,V)$ (Ref. 12).

4 EXACT RIGID-COLUMN SOLUTION

If the time scale of change is of the order of $2D/(f\,V)$, then temporal flow accelerations cannot be ignored. The inertia of the liquid has to be taken into account. The resulting rigid-column equations are:

$$P_1 - P_J = f_1 \frac{L_1}{D_1} \frac{\rho V_1 |V_1|}{2} + \rho L_1 \frac{\mathrm{d}V_1}{\mathrm{d}t} \ ,$$

$$P_J - P_2 = f_2 \frac{L_2}{D_2} \frac{\rho V_2 |V_2|}{2} + \rho L_2 \frac{\mathrm{d}V_2}{\mathrm{d}t} \ ,$$

$$P_J - P_3 = f_3 \frac{L_3}{D_3} \frac{\rho V_3 |V_3|}{2} + \rho L_3 \frac{\mathrm{d}V_3}{\mathrm{d}t} \ ,$$

$$A_1 V_1 = A_2 V_2 + A_3 V_3 \ , \tag{2}$$

where P_1, P_2 and P_3 are given functions of time. This is a system of first-order ordinary differential-algebraic equations (DAEs), which cannot be solved symbolically. Only for special cases, for example the instantaneous starting and stopping of flow, symbolic solutions may be found. For frictionless systems and linear(ised) friction, the equations can be solved exactly. See Refs. (12-13) for a range of symbolic solutions obtained for single-pipe systems.

5 EXACT WATERHAMMER SOLUTION

If the time scale of excitation is in the acoustic range, that is of the order of $4L/c$, with c the Moens-Korteweg speed of sound, then the classical waterhammer equations have to be used (Refs. 17-18):

$$\frac{\partial V_i}{\partial t}+\frac{1}{\rho}\frac{\partial P_i}{\partial x}=-\frac{f_i}{2D_i}V_i\left|V_i\right| \ ,$$

$$\frac{\partial V_i}{\partial x}+\frac{1}{\rho c_i^2}\frac{\partial P_i}{\partial t}=0 \ ,$$

$$A_1 V_{1,\mathrm{J}}=A_2 V_{2,\mathrm{J}}+A_3 V_{3,\mathrm{J}} \ ,$$

$$P_{1,\mathrm{J}}=P_{2,\mathrm{J}}=P_{3,\mathrm{J}} \ , \tag{3}$$

where $V_{i,\mathrm{J}}$ and $P_{i,\mathrm{J}}$ are the velocity and pressure at side i of the junction. The boundary conditions are constant reservoir "pressures" $P_{\mathrm{r}1}$ and $P_{\mathrm{r}3}$, and instantaneous valve closure at Reservoir 2, that is $V_{\mathrm{v}2}$ = 0 at the closed valve. The friction factors in the unsteady calculation are set equal to zero to allow exact solution of the six partial differential equations in (3). The initial conditions for the unsteady calculation are zero "pressures" and constant flow velocities, satisfying the two algebraic equations in (3). The unsteady pressures have to be superposed on top of the steady-state pressures.

The solution of (3) is in terms of the two Riemann invariants (indicated with the subscripts 1 and 2)

$$\eta i_1=V_i+\frac{P_i}{\rho c_i} \quad \text{and} \quad \eta i_2=V_i-\frac{P_i}{\rho c_i} \ , \tag{4}$$

which are constant along the characteristic lines with slopes dx/dt = c_i and dx/dt = $-c_i$ (the index or extension i denotes the pipe number) in the distance-time plane, respectively. The physical boundary and initial conditions, and the final results, are expressed in terms of P_i and V_i and therefore one needs the inverse relations

$$V_i=\frac{1}{2}\left(\eta i_1+\eta i_2\right) \quad \text{and} \quad P_i=\frac{1}{2}\rho c_i\left(\eta i_1-\eta i_2\right) \ . \tag{5}$$

Zero velocity or zero pressure imposed at a boundary give the conditions $\eta i_1=-\eta i_2$ or $\eta i_1=\eta i_2$, respectively.

The exact method of computation is briefly explained for a single pipe, thereby omitting the pipe index i = 1. In boundary point P (in Fig. 3) the Riemann invariant η_1 is given, so that η_2 can be calculated exactly from one constant, linear or quadratic boundary condition at $x = L$. In boundary point Q (in Fig. 3) the Riemann invariant η_2 is given, so that η_1 can be calculated from one boundary condition at x = 0. The Riemann invariant η_2 at Q is computed at point R (in Fig. 3) in precisely the same way as it is calculated at point P. This observation implies that the entire computation can be condensed into one simple recursion, which ends when the initial conditions are "hit". The method is fully explained in Ref. (19). The pseudo-code for a three-reservoir system is given herein in the Appendix. The method also works for non-uniform initial conditions and time-dependent boundary conditions (Refs. 20-21). Friction and damping can be introduced at the boundaries. The main advantage of the method is that a computational grid is not required. In that sense it is a mesh-free method, although different from the traditional meshless methods in Refs. (22-23). In contrast to standard MOC, no interpolations or wave-speed adjustments are needed in multi-pipe systems. The method has successfully been applied to waterhammer with FSI in unbranched systems (Refs. 24-25).

The key equation for the three-reservoir system is the three-way junction condition:

$$\eta1_2 = \eta1_1 - \frac{2\mathcal{A}}{c_1}\ , \qquad \eta2_1 = \eta2_2 + \frac{2\mathcal{A}}{c_2}\ , \qquad \eta3_1 = \eta3_2 + \frac{2\mathcal{A}}{c_3}$$

$$\text{with} \quad \mathcal{A} := \frac{A_1\,\eta1_1 - A_2\,\eta2_2 - A_3\,\eta3_2}{\dfrac{A_1}{c_1} + \dfrac{A_2}{c_2} + \dfrac{A_3}{c_3}}\ . \tag{6}$$

The plus and minus signs in Eq. (6) depend on co-ordinate system and sign convention.

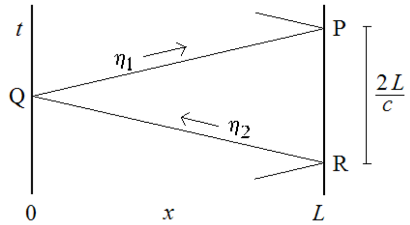

Figure 3. Wave paths and Riemann invariants in distance-time plane.

The meshless method has been successfully applied to frictionless waterhammer in the three-reservoir problem specified in Table 1, which is a combination of previous benchmark problems (Refs. 19 and 25). The fluid is water with density $\rho = 1000$ kg/m^3 and stiffness $K = 2.1$ GPa. The initial situation is constant flow at zero dynamic pressure, although initial pressure-gradients causing linear line pack (Ref. 26) are allowed. The obtained results agree with standard MOC calculations obtained with tiny wave-speed adjustments (less than 0.3%) on a very fine staggered grid (Fig. 4; number of computational reaches N in Pipes 1, 2 and 3: $N_1 = 152$, $N_2 = 352$ and $N_3 = 160$). Pressures and velocities computed with the recursion (see Appendix) are displayed in Fig. 5. At first sight it looks like that the signals contain numerical error or noise. But this is not the case: the shown results are exact. The reason for the whimsical signals is that the number of wave fronts in the system is growing exponentially in time. At the junction, one incident wave results in one reflected wave and two transmitted waves. Waves once generated will not disappear, because the system is frictionless and the computation is exact. In (physical and numerical) practice, dispersion, dissipation and non-instantaneous valve closure will blur spikes and high-frequency fluctuations in pressure and velocity. Nevertheless, what is shown in Fig. 5 is representative of what can be found behind the blurred signal and "surviving" spikes may contribute to "noise" in real systems with flanges, clamps, etc. Figure 6 shows pressure and velocity distributions along the three pipes.

Table 1. Properties of test problem.

pipe (#)	L (m)	D (m)	e (mm)	c (m/s)	V_0 (m/s)
1	10	0.797	16	1184	0.5
2	20	0.797	8	1026	1.0
3	10	0.797	12	1123	–0.5

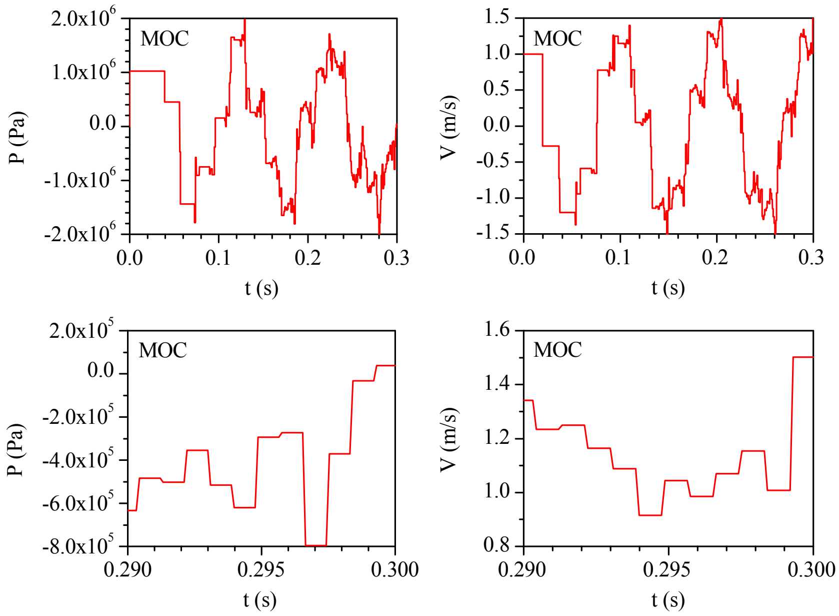

Figure 4. Standard MOC results obtained on very fine computational grid.
Pressure at valve (left) and velocity at junction in Pipe 2 (right).
Top figures: full history. Bottom figures: last 0.01 seconds.

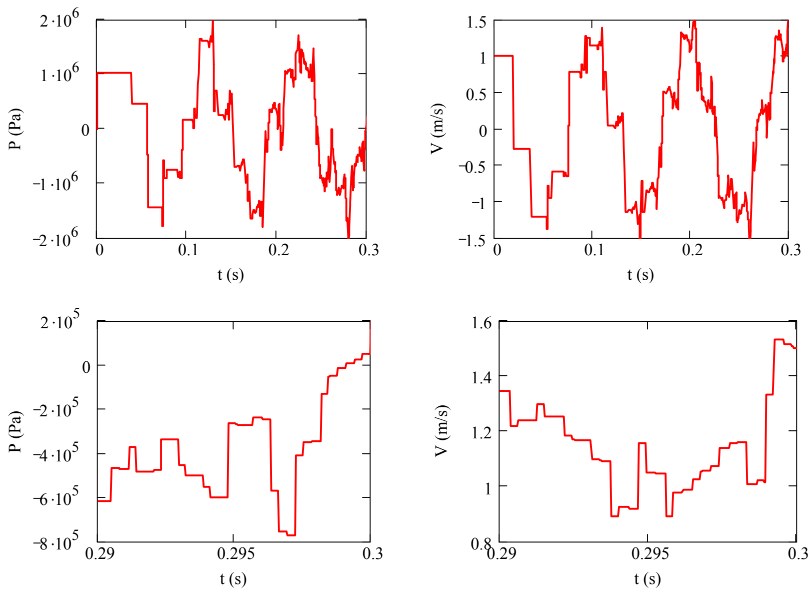

Figure 5. Exact solution.
Pressure at valve (left) and velocity at junction in Pipe 2 (right).
Top figures: full history (600 points). Bottom figures: last 0.01 seconds (300 points).

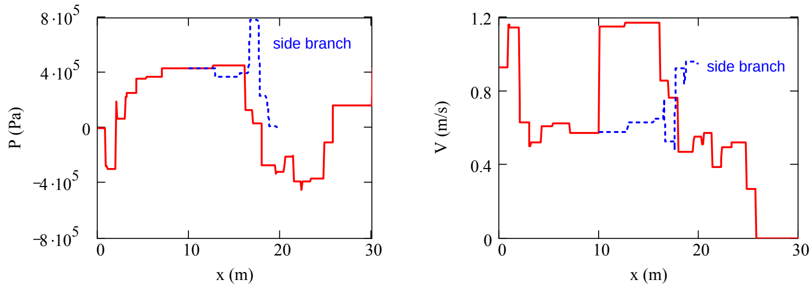

Figure 6. Pressure and velocity distribution along the three pipes at *t* = 0.1 s (500 points).

The obtained results give rise to a few interesting academic questions. The solutions are piecewise constant, but it is not known whether they are constant in between two computed points or not. The number of travelling discontinuities is growing exponentially in time (according to Fibonacci-type sequences). Will the limit solution for infinite time be a continuous or a fractal-type function? Will the solution become smoother or spikier? Is there a chance that a Dirac pulse develops as the result of repeated positive wave superposition (like Maxwell's demon)? Does the central limit theorem apply? What is the regularity of the final solution? It is impossible to numerically compute solutions for large times and large resolutions, so profound mathematical methods are required to give answers here.

6 CONCLUSION

Exact computation of frictionless waterhammer in a three-reservoir system has been achieved by one recursion including all three pipes. The mesh-free method has been verified against conventional waterhammer results obtained on a very fine computational grid. The method is able to detect all of the exponentially growing number of wave fronts. This scenario is a nightmare for most if not all alternative numerical schemes. The obtained solutions can serve as a benchmark for testing numerical methods.

REFERENCES

(1) Coriolis G. (1838) Calcul des effets de la machine à élever de l’eau, au moyen des oscillations, de l’invention de M. de Caligny. Journal de Mathématiques Pures et Appliquées, Tome III, 437-459.

(2) Coriolis G. (1838) Rapport sur un Mémoire de M. de Caligny, ayant pour objet la description d'une machine de son invention, destinée à élever de l’eau à l'aide des oscillations. Compte Rendu des Séances de l'Académie des Sciences, 20 August 1838, 419-425.

(3) de Caligny A. (1838) Sur le calcul des effets de la Machine précédente et les dispositions essentielles de ses tuyaux d'ascension. – Coup d'œil historique sur quelques machines à élever l'eau. Journal de Mathématiques Pures et Appliquées, Tome III, 460- 476, 624-625.

(4) de Caligny A. (1838) Sur la Théorie des oscillations de l'eau dans les tuyaux de conduite. Journal de Mathématiques Pures et Appliquées, Tome III, 209-234.

(5) Tacke J.H.P.M. (1988) Hydraulic rams – a comparative investigation. Communications on Hydraulic and Geotechnical Engineering, Delft University of Technology, Faculty of Civil Engineering, Report 88-1, ISSN 0169-6548; available from TU Delft repository: http://repository.tudelft.nl/

(6) Glover P.B.M., Boldy A.P. (1989) Computer simulation of the hydraulic ram pump. BHRA, Proc. of the 6th Int. Conf. on Pressure Surges (Editor A.R.D. Thorley), Cambridge, United Kingdom, October 1989, pp. 333-340.

(7) Tacke J.H.P.M., Verspuy C. (1989) Hydraulic rams. World Pumps, July issue, 200-203.

(8) Verspuy C., Tijsseling A.S. (1993) Hydraulic ram analysis. IAHR Journal of Hydraulic Research 31, 267-278.

(9) Najm H.N., Azoury P.H., Piasecki M. (1999) Hydraulic ram analysis: a new look at an old problem. Journal of Power and Energy, Proc. IMechE 213 Part A, 127-141.

(10) Filipan V., Virag Z., Bergant A. (2003) Mathematical modelling of a hydraulic ram pump system. Journal of Mechanical Engineering / Strojniški vestnik 49(3), 137-149.

(11) Jaeger C. (1977) Fluid Transients in Hydro-Electric Engineering Practice. Glasgow and London: Blackie.

(12) Tijsseling A.S., Vardy A.E. (2004) Time scales and FSI in unsteady liquid-filled pipe flow. BHR Group, Proc. of the 9th Int. Conf. on Pressure Surges (Editor S.J. Murray), Chester, United Kingdom, March 2004, pp. 135-150.

(13) Tijsseling A.S., Vardy A.E. (2008) Time scales and FSI in oscillatory liquid-filled pipe flow. BHR Group, Proc. of the 10th Int. Conf. on Pressure Surges (Editor S. Hunt), Edinburgh, United Kingdom, May 2008, pp. 553-568.

(14) Sathuraman S., Rangaraju K.G. (1969) Direct solution of three-reservoir problem. Civil Engineering Journal 11, April issue, paper no CE 143.

(15) Singh R. (1982) Direct solution of three-reservoir problem. Journal of the Institution of Engineers (India): Civil Engineering Division, 62(5), 292-296.

(16) Loganathan G.V., Kuo C.Y. (1985) A direct solution for the classical three reservoir problem. Civil Engineering for Practicing and Design Engineers 4, 1-11.

(17) Wylie E.B., Streeter V.L. (1993) Fluid Transients in Systems. Englewood Cliffs: Prentice Hall.

(18) Chaudhry M.H. (1987) Applied Hydraulic Transients (2nd edition). New York: Van Nostrand Reinhold.

(19) Tijsseling A.S., Bergant A. (2007) Meshless computation of water hammer. Proc. of the 2nd IAHR Int. Meeting of the Workgroup on Cavitation and Dynamic Problems in Hydraulic Machinery and Systems (Editors R. Susan-Resiga, S. Bernad, S. Muntean), Timişoara, Romania, October 2007, Scientific Bulletin of the "Politehnica" University of Timişoara, Transactions on Mechanics, Vol. 52(66), No. 6, pp. 65-76, ISSN 1224-6077.

(20) Tijsseling A.S., Hou Q., Svingen B., Bergant A. (2010) Acoustic resonance in a reservoir-pipeline-orifice system. Proc. of the ASME 2010 Pressure Vessels and Piping Division Conf., Bellevue, Washington, USA, July 2010, Paper PVP2010-25083.

(21) Tijsseling A.S., Hou Q., Svingen B., Bergant A. (2012) Acoustic resonance in a reservoir - double pipe - orifice system. Proc. of the ASME 2012 Pressure Vessels and Piping Division Conf., Toronto, Canada, July 2012, Paper PVP2012-78085.

(22) Hou Q.Z., Kruisbrink A.C.H., Tijsseling A.S., Keramat A. (2012) Simulating water hammer with corrective smoothed particle method. BHR Group, Proc. of the 11th Int. Conf. on Pressure Surges (Editor Sandy Anderson), Lisbon, Portugal, October 2012, pp. 171-187.

(23) Zhang G.M., Batra R.C. (2004) Modified smoothed particle hydrodynamics method and its application to transient problems. Computational Mechanics 34, 137–146.

(24) Tijsseling A.S. (2003) Exact solution of linear hyperbolic four-equation systems in axial liquid-pipe vibration. Journal of Fluids and Structures 18, 179-196.

(25) Tijsseling A.S. (2009) Exact computation of the axial vibration of two coupled liquid-filled pipes. Proc. of the 2009 ASME Pressure Vessels and Piping Division Conf., Prague, Czech Republic, July 2009, Paper PVP2009-77250.

(26) Vardy A.E., Fan, D. (1987) Constitutive factors in transient internal flows. Proc. of the Int. Conf. on Numerical Methods in Engineering: Theory and Applications (NUMETA 87), Swansea, United Kingdom, Vol. 2, Paper T37.

APPENDIX Recursion for three-reservoir system

<u>*Boundary and junction points*</u>

The recursion BOUNDARY calculates the Riemann invariants ηi_1 and ηi_2 defined in Eq. (4) and placed in the vectors $\boldsymbol{\eta 1} = (\eta 1_1, \eta 1_2)^T$, $\boldsymbol{\eta 2} = (\eta 2_1, \eta 2_2)^T$ and $\boldsymbol{\eta 3} = (\eta 3_1, \eta 3_2)^T$ for the Pipes 1, 2 and 3, respectively, in the boundary and junction points (finally) from constant initial values $\boldsymbol{\eta 1}_0$, $\boldsymbol{\eta 2}_0$ and $\boldsymbol{\eta 3}_0$. Here $L = L_1 + L_2$. The x coordinate of Pipe 3 starts at L. The position of the junction is $x_J = L_1$. The pseudo-code reads:

BOUNDARY (<u>input</u>: x, t; <u>output</u>: $\boldsymbol{\eta 1}, \boldsymbol{\eta 2}, \boldsymbol{\eta 3}$)
if $(t \le 0)$ then
    $\boldsymbol{\eta 1} := \boldsymbol{\eta 1}_0$
    $\boldsymbol{\eta 2} := \boldsymbol{\eta 2}_0$
    $\boldsymbol{\eta 3} := \boldsymbol{\eta 3}_0$
else
    if $(x = 0)$ then
        CALL BOUNDARY $(x_J,\ t - L_1 / c_1 ; \boldsymbol{\eta 1}, \boldsymbol{\eta 2}, \boldsymbol{\eta 3})$
        $\eta 1_1 := \eta 1_2$
    if $(x = L)$ then
        CALL BOUNDARY $(x_J,\ t - L_2 / c_2 ; \boldsymbol{\eta 1}, \boldsymbol{\eta 2}, \boldsymbol{\eta 3})$
        $\eta 2_2 := -\eta 2_1$
    if $(x = L + L_3)$ then
        CALL BOUNDARY $(x_J,\ t - L_3 / c_3 ; \boldsymbol{\eta 1}, \boldsymbol{\eta 2}, \boldsymbol{\eta 3})$
        $\eta 3_2 := \eta 3_1$
    if $(x = x_J)$ then
        CALL BOUNDARY $(0,\ t - L_1 / c_1 ; \boldsymbol{\eta 1}, \boldsymbol{\eta 2}, \boldsymbol{\eta 3})$
        $\eta 1 := \eta 1_1$
        CALL BOUNDARY $(L,\ t - L_2 / c_2 ; \boldsymbol{\eta 1}, \boldsymbol{\eta 2}, \boldsymbol{\eta 3})$
        $\eta 2 := \eta 2_2$

CALL BOUNDARY ($L + L_3$, $t - L_3 / c_3$; **η1**, **η2**, **η3**)
$\eta 3 := \eta 3_2$
$$\mathcal{A} := \frac{A_1 \eta 1_1 - A_2 \eta 2_2 - A_3 \eta 3_2}{\frac{A_1}{c_1} + \frac{A_2}{c_2} + \frac{A_3}{c_3}} \qquad \text{(Eq. 6)}$$
$\eta 1_1 := \eta 1$
$\eta 1_2 := \eta 1 - 2\mathcal{A} / c_1$
$\eta 2_1 := \eta 2 + 2\mathcal{A} / c_2$
$\eta 2_2 := \eta 2$
$\eta 3_1 := \eta 3 + 2\mathcal{A} / c_3$
$\eta 3_2 := \eta 3$
end

Interior points
The subroutine INTERIOR calculates **η1**, **η2** and **η3** in the interior points from the boundary and junction values. The pseudo-code reads:

INTERIOR (input: x, t; output: **η1**, **η2**, **η3**)
if $(0 < x < x_J)$ then
CALL BOUNDARY (0, $t - x / c_1$; **η1**, **η2**, **η3**)
$\eta 1 := \eta 1_1$
CALL BOUNDARY (x_J, $t - (x_J - x) / c_1$; **η1**, **η2**, **η3**)
$\eta 2 := \eta 1_2$
$\eta 1_1 := \eta 1$
$\eta 1_2 := \eta 2$
if $(x_J < x < L)$ then
CALL BOUNDARY (x_J, $t - (x - x_J) / c_2$; **η1**, **η2**, **η3**)
$\eta 1 := \eta 2_1$
CALL BOUNDARY (L, $t - (L - x) / c_2$; **η1**, **η2**, **η3**)
$\eta 2 := \eta 2_2$
$\eta 2_1 := \eta 1$
$\eta 2_2 := \eta 2$
if $(L < x < L_3)$ then
CALL BOUNDARY (x_J, $t - (x - L) / c_3$; **η1**, **η2**, **η3**)
$\eta 1 := \eta 3_1$
CALL BOUNDARY ($L + L_3$, $t - (L + L_3 - x) / c_3$; **η1**, **η2**, **η3**)
$\eta 2 := \eta 3_2$
$\eta 3_1 := \eta 1$
$\eta 3_2 := \eta 2$
end